World Academy of Science, Engineering and Technology
International Journal of Aerospace and Mechanical Engineering
Vol:12, No:12, 2018

Compressible Lattice Boltzmann Method for Turbulent Jet Flow Simulations

K. Noah, F.-S. Lien

***Abstract*—**In Computational Fluid Dynamics (CFD), there are a variety of numerical methods, of which some depend on macroscopic model representatives. These models can be solved by finite-volume, finite-element or finite-difference methods on a microscopic description. However, the lattice Boltzmann method (LBM) is considered to be a mesoscopic particle method, with its scale lying between the macroscopic and microscopic scales. The LBM works well for solving incompressible flow problems, but certain limitations arise from solving compressible flows, particularly at high Mach numbers. An improved lattice Boltzmann model for compressible flow problems is presented in this research study. A higher-order Taylor series expansion of the Maxwell equilibrium distribution function is used to overcome limitations in LBM when solving high-Mach-number flows. Large eddy simulation (LES) is implemented in LBM to simulate turbulent jet flows. The results have been validated with available experimental data for turbulent compressible free jet flow at subsonic speeds.

***Keywords*—**Compressible lattice Boltzmann metho-, large eddy simulation, turbulent jet flows.

I. Introduction

THE LBM is a relatively new approach as an alternative numerical method for modeling physical phenomena in fluid flows. It was originally developed from the lattice gas automata method (LGA) [1], which can be constructed as a simplified fictitious molecular dynamics model in which space, time, and particle velocities are all discrete [2]. LBM is known to be a new powerful tool to simulate various incompressible flows. However, LBM has also been found with a significant limitation in solving high-Mach-number compressible flows. The major cause of this limitation is the contraction in the Maxwellian distribution function, which should be in the polynomial form of particle velocity [3]. So the truncated equilibrium distribution function inevitably limits the range of the applicable Mach number. In the literature, there have been many recent successful models reported to solve compressible flow problems using LBM. Shouxin et al. [4] introduced two lattice models: D2Q13 and D3Q17, which depend on three energy levels for the density distribution function. The difficulty of using these two models is that there are many parameters in the models which were chosen based on physical concepts. Shan and He [5] introduced a new model for compressible LBM using a third-order Maxwell-Boltzmann equilibrium distribution function to reduce the truncation error and demonstrated success in solving compressible flow problems with Mach numbers up to $M_\infty = 0.6$. Other researchers proposed to develop alternative equilibrium distribution functions instead of higher-order Maxwell-Boltzmann equilibrium distribution functions. For example, Kataoka and Tsutahara [6], [7] presented two compressible LBM models based on the specific heat energy which cannot be chosen freely and introduced a new coefficient to control the specific-heat at any location on a lattice grid. Qu et al. [8] proposed a novel method of replacing the Maxwell-Boltzmann equilibrium distribution function with a circular lattice distribution function, which is a probability distribution of a random variable in terms of angle. In this model, they avoided the truncation error due to the use of the Maxwell-Boltzmann distribution equation and increased the range of applicable Mach number in LBM to the supersonic flow regimes.

Khalid Noah. Department of Mechanical and Mechatronics Engineering, University of Waterloo, Waterloo, 200 University Avenue West, Waterloo, ON, Canada, N2L 3G1 (phone: +1519-888-4567 x38840; e-mail: knoah@ uwaterloo.ca).

Fue-Sang Lien. Department of Mechanical and Mechatronics Engineering, University of Waterloo, Waterloo, 200 University Avenue West, Waterloo, ON, Canada, N2L 3G1 (phone: +1519-888-4567 x36528, Fax: +1519-885-5862; e-mail: knoah@uwaterloo.ca)

II. Lattice Boltzmann Method

The Boltzmann equation for a system without an external force can be expressed as:

$$\frac{\partial f_i}{\partial t} + \vec{c}_i \,.\nabla f_i = \Omega \tag{1}$$

where Ω the is collision operator, f_i is the distribution function and $\vec{c}_i$ is the lattice speed.

Bhatnagar, Gross and Krook (BGK) [9] proposed a model for the collision operator in the Boltzmann equation as:

$$\Omega = \omega\left(f^{eq}{}_i - f_i\right) = \frac{\Delta t}{\tau}\left(f^{eq}{}_i - f_i\right) \tag{2}$$

where $\omega = \frac{\Delta t}{\tau}$ in (2), ω is the collision frequency, τ is the relaxation factor, Δt is the time and f^{eq} is the local equilibrium distribution function.

Now we can rewrite the Boltzmann equation in a specific particle velocity direction as:

$$\frac{\partial f_i}{\partial t} + \vec{c}_i.\nabla f_i = \frac{\Delta t}{\tau}(f^{eq}{}_i - f_i) \tag{3}$$

And this equation can be discretized in space and time as:

$$f_i\,(x + \vec{c}_i\Delta t, t + \Delta t) = f_i(x,t) + \frac{\Delta t}{\tau}[f_i^{eq}(x,t) - f_i(x,t)] \tag{4}$$

As we can see, the beauty of this equation lies in its simplicity, and it can be applied to many fluid mechanics problems. The Maxwell–Boltzmann distribution is a statistical probability distribution. It is used to describe particle speeds for ideal gases, where the particles move freely inside a stationary container. The interaction between particles is neglected, except for very brief collisions. These collisions lead to a very small change in the energy and momentum within the environment. A good choice of the equilibrium distribution function is the key for applying LBM to a wide range of fluid flow problems in different conditions [10]. The implication of this is that different equilibrium distribution functions may be required in compressible LBM than for incompressible LBM. An expansion of the Maxwell-Boltzmann distribution up to 2nd-order in velocities gives us:

$$f_i^{eq}(x,t) = \omega_i \rho \left(1 + \frac{\vec{c}_i.\vec{u}}{c_s^2} + \frac{(\vec{c}_i.\vec{u})^2}{2c_s^4} - \frac{\vec{u}^2}{2c_s^2}\right) + O(\vec{u}^3) \quad (5)$$

where $c_s = \frac{c_k}{\sqrt{3}}$ is the sound speed and ω is the lattice weight factor.

III. Compressible Lattice Boltzmann Method

In conventional LBM for solving incompressible flow, the 2nd-order truncation of the Hermite expansion is commonly used to integrate the equilibrium distribution function in the discrete particle velocity space. Shan and Chen [11] used a 3rd-order expansion of the equilibrium distribution function together with the BGK collision term. They also proved that the discretization of the continuum distribution function into values at the nodes (or abscissas) of a quadrature formula is equivalent to the truncation of the higher-order terms in the Hermite spectral space. We can extend Shan & He's model by including up to the 5th-order terms in the Taylor expansion of the Maxwell-Boltzmann equilibrium distribution function as shown below:

$$\begin{aligned} f_i^{eq}(\vec{x},t) = {} & \omega_i\rho\Big\{1 + c_{i\alpha}.u_{i\alpha} + \tfrac{1}{2}\left[(c_{i\alpha}.u_{i\alpha})^2 - u_{i\alpha}^2\right] + \\ & \tfrac{(T-1)}{2}\left(c_{i\alpha}^2 - D\right) + \tfrac{c_{i\alpha}.u_{i\alpha}}{6}\left[(c_{i\alpha}.u_{i\alpha})^2 - 3u_{i\alpha}^2\right] + \\ & \tfrac{T-1}{2}(c_{i\alpha}.u_{i\alpha})\left(c_{i\alpha}^2 - D - 2\right) + \\ & \tfrac{1}{24}\left[(c_{i\alpha}.u_{i\alpha})^4 - 6(c_{i\alpha}.u_{i\alpha})^2u_{i\alpha}^2 + 3u_{i\alpha}^2\right] + \tfrac{T-1}{4}\left[\left(c_{i\alpha}^2 - D - \right.\right. \\ & \left.\left.2\right)\left((c_{i\alpha}.u_{i\alpha})^2 - u_{i\alpha}^2\right) - 2(c_{i\alpha}.u_{i\alpha})^2\right] + \tfrac{(T-1)^2}{8}\left[c_{i\alpha}^4 - \right. \\ & \left.2(D+2)c_{i\alpha}^2 + D(D+2)\right] + \\ & \tfrac{u_{i\alpha}}{120}\left[(c_{i\alpha}.u_{i\alpha})^4 - 10(c_{i\alpha}.u_{i\alpha})^2u_{i\alpha}^2 + 15u_{i\alpha}^5\right] + \tfrac{T-1}{12}u_{i\alpha}\left[\left(c_{i\alpha}^2 - \right.\right. \\ & \left.\left.D - 4\right)(c_{i\alpha}.u_{i\alpha})^2 - u_{i\alpha}^2\right) - 2(c_{i\alpha}.u_{i\alpha})^2] + \tfrac{(T-1)^2}{8}u_{i\alpha}[c_{i\alpha}^4 - \\ & 2(D+2)c_{i\alpha}^2 + (D+2)(D+4)]\Big\}, \end{aligned} \quad (6)$$

where α denotes the spatial directions in Cartesian coordinates, D is the spatial dimension, T is the temperature, u is the fluid velocity, ρ is the fluid density.

The macroscopic variables are obtained from mass conservation, momentum conservation, and the equation of state, respectively:

$$\rho = \sum_i f_i \quad (7)$$

$$\rho u = \sum_i f_i \vec{c}_i \quad (8)$$

$$P = \rho c_s^2 \quad (9)$$

IV. Subgrid Scale Modeling of Turbulent Flows Using LBM

The LBM has become one of the most popular numerical tools for simulating fluid flow because of its simplicity, applicability in parallel computing and the ease of solving complex geometries. In the past few years, LBM was used only as a direct numerical simulation method. Thus LBM was restricted to solving relatively low-Reynolds-number flows. To solve highly turbulent flows, we have to implement a LES subgrid-scale (SGS) model in LBM. The main idea behind the SGS is to include all the physical effects the unresolved eddy motion has on the resolved fluid motion. To model the unresolved scales of motion at high Reynolds numbers, SGS models are often employed. The SGS models for LES define the formalism of an effective eddy-viscosity model. In order to apply the SGS model in LBM a special filtering operation $\varpi(x)$ is required and it is often introduced as:

$$\varpi(x) = \int \omega(x) G(x,\acute{x}) d\acute{x} \quad (10)$$

where ϖ is a spatially dependent quantity. It can represent density, velocity or any other physical quantity. G is a spatial filter kernel function defined as follows:

$$G_i(x_i, x_i') = \begin{cases} \frac{1}{\Delta_i} \; for \; |x_i - x_i'| < \frac{\Delta_i}{2}, \\ 0 \qquad otherwise, \end{cases} \quad (11)$$

where Δ_i is the filter width.

The most popular subgrid model is the Smagorinsky model [12], where the anisotropic part of the Reynolds stress term is modeled as:

$$\tau_{ij} - \tfrac{\delta_{ij}}{3}\tau_{kk} = -2v_t\bar{S}_{ij} = 2C^2\Delta^2|\bar{S}|\bar{S}_{ij} \quad (12)$$

in which δ_{ij} is the Kronecker delta function, C is the Smagorinsky constant, Δ is the filter width, and $\bar{S}_{ij}$ is the magnitude of the large-scale strain rate tensor:

$$|\bar{S}| = \sqrt{2\bar{S}_{ij}\,\bar{S}_{ij}}. \quad (13)$$

Similarly, we can write the filtered particle distribution function $\bar{f}_\alpha$.

$$\bar{f}_\alpha(x) = \int f_\alpha(x) G(x,x') dx'. \quad (14)$$

In the LES model, we write the filtered lattice Boltzmann equation with the BGK collision model into the following form:

$$\frac{\bar{f}_\alpha(x+e_{\alpha x}\delta_t, y+e_{\alpha y}\delta_t, t+\delta_t)-\bar{f}_\alpha(x,y,t)}{\delta_t} = \frac{\bar{f}_\alpha^{eg}(x,y,t)-\bar{f}_\alpha(x,y,t)}{\tau^*} \quad (15)$$

Equation (15) is similar to the lattice Boltzmann equation except with different relaxation time τ^* defined as:

$$\tau^* = \tau + \tau_t, \quad (16)$$

where τ^* is the total effective relaxation time dependent on the turbulent eddy viscosity, τ is the laminar relaxation time and τ_t is the turbulent relaxation time.

The total viscosity is

$$v^* = v + v_t, \quad (17)$$

where v is the laminar viscosity $v = (\tau - \frac{1}{2})c_s^2\delta t$, and v_t is the turbulent viscosity $v_t = C^2\Delta^2\bar{S}_{ij}$. Now, the total effective relaxation time becomes:

$$\tau_* = \tau + \frac{C^2\Delta^s}{c_s^2\delta t}|\bar{S}|. \quad (18)$$

Using a uniform grid $c_k = \frac{\delta x}{\delta t} = 1$, leading to $c_s^2 = 1/3$. This in turn gives

$$\tau_* = \frac{|\bar{Q}|}{2\rho c_s^2|\bar{S}|}, \quad (19)$$

where the non-equilibrium stress tensor invariant $|\bar{S}|$ is given as:

$$Q = \sum_\alpha c_{\alpha i}c_{\alpha j}(\bar{f}_\alpha - \bar{f}_\alpha^{eq}), \quad (20)$$

$$|\bar{S}|^2 + \frac{\tau\,\delta t\,c_s^2}{C^2\Delta^2}|\bar{S}| - \frac{\delta t\,|\bar{Q}|}{2\rho C^2\Delta^2} = 0 \quad (21)$$

We solving (21) for $|\bar{S}|$ and substituting the positive solution of $|\bar{S}|$ into (18) to obtain the total effective relaxation time τ_* as:

$$\tau_* = \frac{1}{2}\left(\sqrt{\tau^2 + \frac{2C^2\Delta^2}{\rho\, c_s^4\,\delta t}|\bar{Q}|} - t\right). \quad (22)$$

V. Results and Discussion

In this case study, where the Reynolds number is high, the results will be validated against the experimental data for a square jet at different locations along the jet centerline $(0 < X/D < 4)$, where the streamwise velocity is almost constant, and Reynolds number plays a main role in the jet development. The mean velocity along the jet centerline and the cross-section velocity profile at different distances from the jet exit U_j will be compared with experimental results. Fig. 1 shows the schematic of the square jet nozzle and the reference system where U_c is the local centerline velocity, and u_x is the instantaneous streamwise velocity at any (y, z) location.

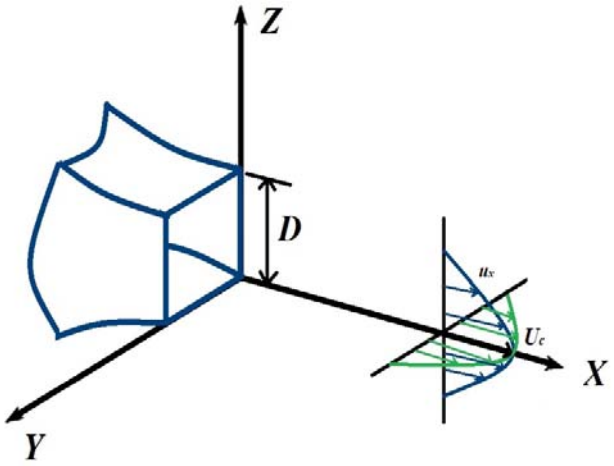

Fig. 1 Schematic of a square jet nozzle and the reference system

The evolution of mean velocity distributions and the streamwise turbulent intensity at $X/D = 0.5$ along with the experimental results from Ghasemi [13] are shown in Fig. 2. The mean jet velocity and the turbulent intensity are normalized to the jet exit velocity at the centerline which is the maximum mean velocity $U_{max}(x)$. The results in Fig. 2 (a) show that there is no effect from the free shear layer, so the mean velocity will be constant and equal to the jet exit velocity. Fig. 2 (b) shows turbulence intensity distributions, which mainly depend on the Reynolds number [14]. These distributions appear to decrease with an increase in the Reynolds number. The turbulent intensity is confined to the jet centerline region, where there are no effects from the mixing shear layer yet.

Fig. 3 shows the spanwise velocity profiles of the mean streamwise velocity at different locations along the jet axial direction (X/D =1,2,3,4, and 5) in the near-field region of the square jet. In Fig. 3 (a) ($X/D = 1$) the flow is not affected by nearby free shear layer, and the velocity is almost constant between ($Y/D = 0$) and ($Y/D = 0.4$), which is equal to the jet exit velocity U_j. When moving a little bit farther from the jet exit in Figs. 3 (b), (c) ($X/D = 2$ and $X/D = 3$), the free shear layer has some effect on the jet core flow and the velocity starts to resemble the Gaussian profile. But it still has a flat hat at ($Y/D = 0 - 0.3$). When moving to the end of the near-field flow region at ($X/D = 4 - 5$) as shown in Figs. 3 (d), (e), the flow is fully developed and the velocity has a top-hat distribution. In general, the mean streamwise velocity profiles u_x/U_j decreases along the jet X-axis and in the radial direction away from the jet centerline, where free shear layers and mixing layers created turbulent flow region. These figures indicate that there is a good agreement at all locations along the streamwise direction between the experimental and LBM-LES results.

In conclusion, a LBM to solve compressible turbulent flow by using a higher-order distribution function and combined LBM with a LES SGS model to simulate a free jet at subsonic flow regime has been developed. The essential idea of applying LES in LBM is to define a space-filtered particle

distribution and to allow the dynamics of the filtered particle distribution to have a space-dependent relaxation. The LBM-LES results compare well with the experimental data in terms of the mean streamwise velocity and the turbulent intensity at different downstream locations and the spreading rate of the jet. The LBM for compressible flows is still under development in the research community, and it can be an exciting research area with many possible applications.

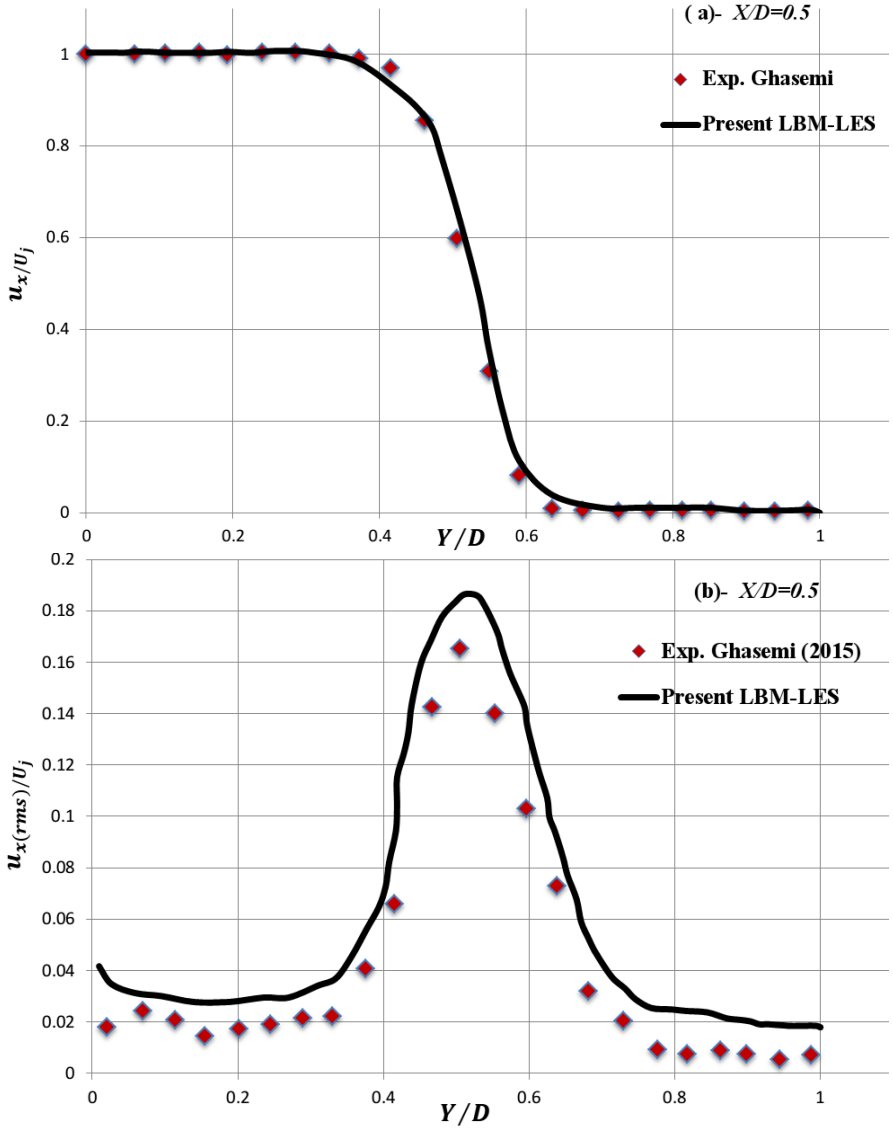

Fig. 2 (a) The spanwise distribution of mean streamwise velocity u_x/U_j. (b) The streamwise turbulence intensity $u_{x(rms)}/U_j$

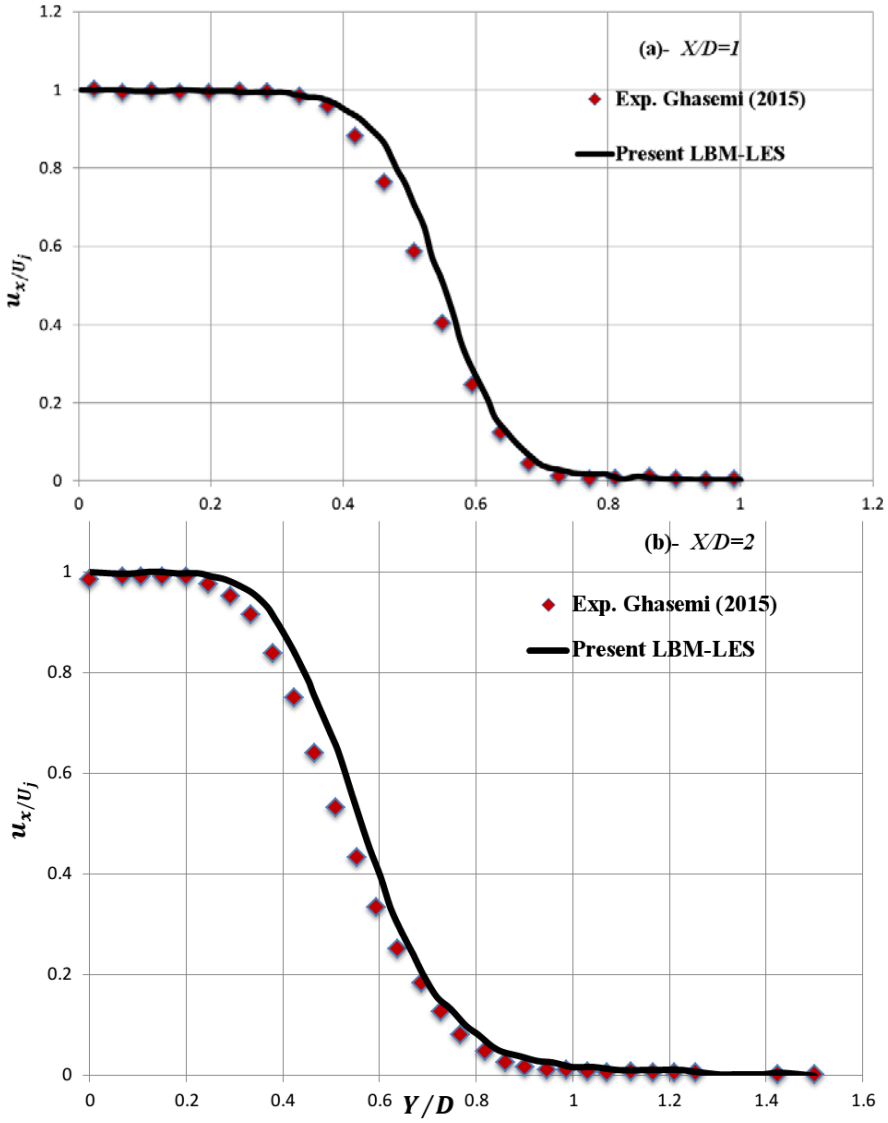

Fig. 3 (a) (b) The mean streamwise velocity profiles of the square jet at different locations along the jet X-axis

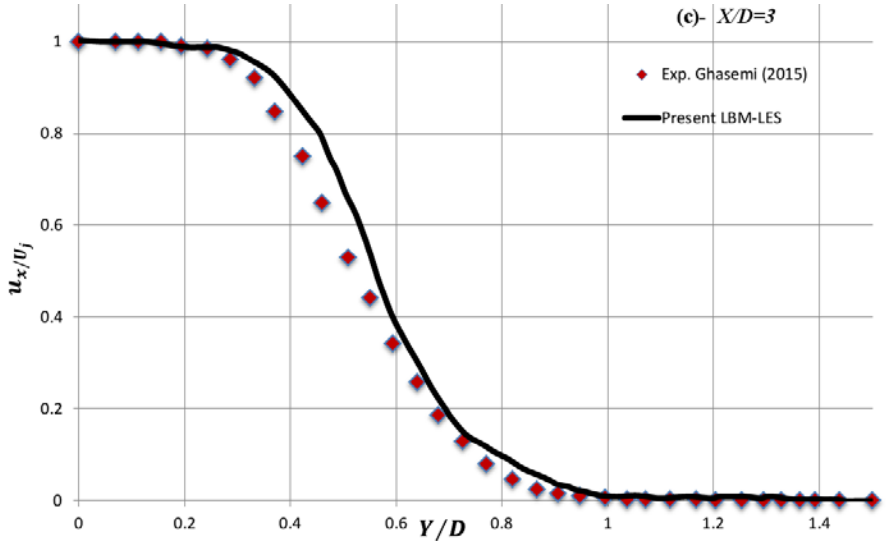

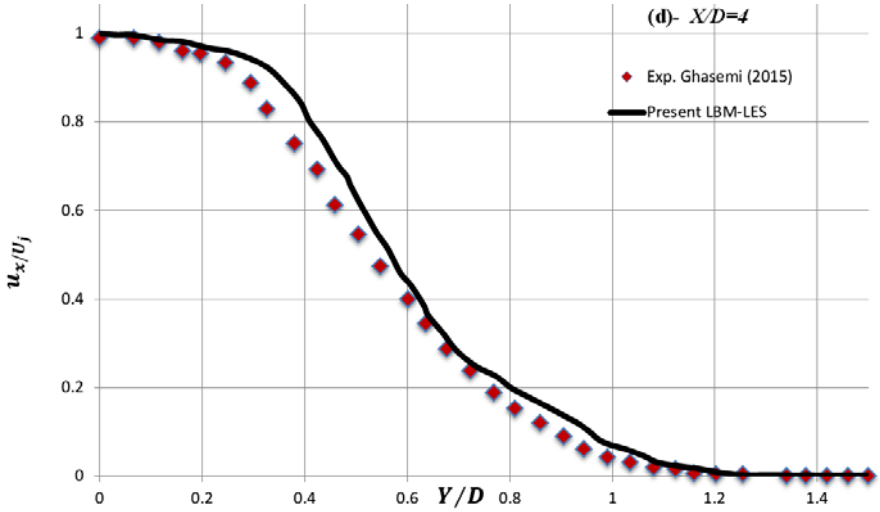

Fig. 3 (c), (d) The mean streamwise velocity profiles of the square jet at different locations along the jet X-axis

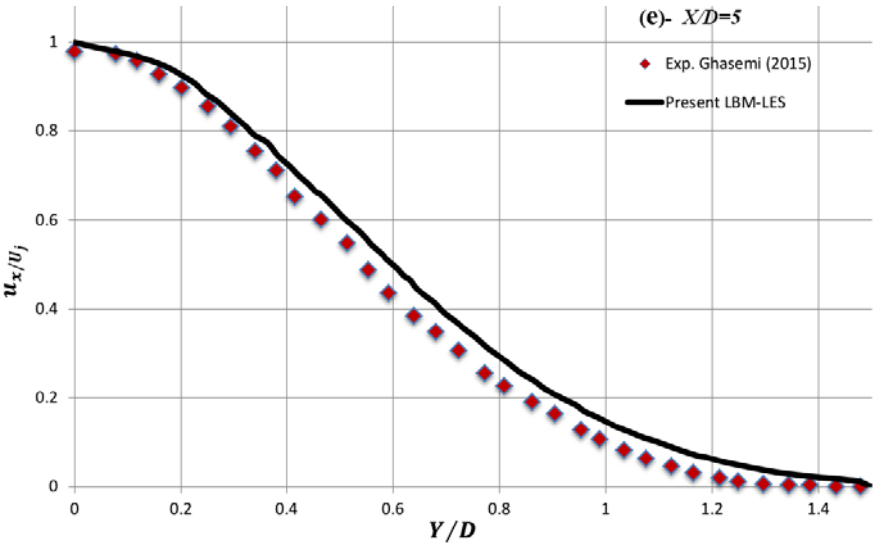

Fig. 3 (e) The mean streamwise velocity profiles of the square jet at different locations along the jet X-axis

REFERENCES

[1] A. Dieter and Wolf-Gladrow, Lattice-gas cellular automata and lattice Boltzmann models: An introduction. Berlin: Springer-Verlag Berlin and Heidelberg GmbH & Co. K, 2002.

[2] J. Tu, C. Liu, and G. Yeoh, Computational Fluid Dynamics: A Practical Approach.: Butterworth-Heinemann, 2013.

[3] Z. Guo and C. Shu, Lattice Boltzmann method and its applications in engineering. Singapore: World Scientific, 2013.

[4] H. Shouxin, Y. Guangwu, and H. Weiping, "A lattice Boltzmann model for compressible perfect gas," Acta Mechanica Sinica, vol. 13, no. 3, pp. 218-226, Aug. 1997.

[5] X. Shan and X. He, "Discretization of the velocity space in the solution of the Boltzmann equation," Physical Review Letters, vol. 80, no. 1, pp. 65-68, Jan. 1998.

[6] T. Kataoka and M. Tsutahara, "Lattice Boltzmann method for the compressible Euler equations," Physical Review E, vol. 69, no. 5, May 2004a.

[7] T. Kataoka and M. Tsutahara, "Lattice Boltzmann model for the compressible Navier-Stokes equations with flexible specific-heat ratio," Physical Review E, vol. 69, no. 3, Mar. 2004b.

[8] K. Qu, C. Shu, and Y.T. Chew, "Alternative method to construct equilibrium distribution functions in lattice-Boltzmann method simulation of inviscid compressible flows at high Mach number," Physical Review E, vol. 75, no. 3, Mar. 2007.

[9] P. L. Bhatnagar, E. P. Gross, and M. Krook, "A model for collision processes in gases. I. Small amplitude processes in charged and neutral One-Component systems," Physical Review, vol. 94, no. 3, pp. 511-525, May 1954.

[10] D. Oztekin, "The Lattice Boltzmann Methods and Their Applications to Fluid Flows," Lehigh University, Thesis 2014.

[11] X. Shan and H. Chen, "Lattice Boltzmann model for simulating flows with multiple phases and components," Physical Review E, vol. 47, no. 3, pp. 1815-1819, Mar. 1993.

[12] J. Smagorinsky, "General Circulation Experiments With The Primitive Equations," Monthly Weather Review, vol. 91, no. 3, pp. 99-164, March 1963.

[13] A. Ghasemi, V. Roussinova, R. Balachandar, and R.M. Barron, "Reynolds number effects in the near-field of a turbulent square jet," Experimental Thermal and Fluid Science, vol. 61, pp. 249-258, Feb. 2015.

[14] H. Yu, L. Luo, and S. Girimaji, "LES of turbulent square jet flow using an MRT lattice Boltzmann model," Computers & Fluids, vol. 35, no. 8-9, pp. 957-965, Sep. 2006.